(4) Flory, P. J. *Macromolecules* **1978**, *11*, 1141.
(5) Maier, W.; Saupe, A. *Z. Naturforsch.* **1959**, *149*, 882; *Z. Naturforsch.* **1960**, *159*, 187.
(6) Dalmolen, L. G. P.; Picken, S. J.; De Jong, A. F.; De Jeu, W. H. *J. Phys.* **1985**, *46*, 1443.
(7) Ying, Q.; Chu, B. *Makromol. Chem., Rapid Commun.* **1984**, *5*, 785.
(8) Cotter, M. A. *Mol. Cryst. Liq. Cryst.* **1977**, *39*, 173.
(9) Luckhurst, G. R. In *Molecular Physics of Liquid Crystals*; Luckhurst, G. R.; Gray, G. W., Eds.; Academic: London, 1979; pp 85–119.
(10) Jähnig, F. *J. Chem. Phys.* **1979**, *70*(7), 3279.
(11) Warner, M.; Gunn, J. M. F.; Baumgartner, A. *J. Phys.* **1985**, *18*(A), 3007.
(12) Cifferi, A.; Marsano, E. *Gazz. Chim. Ital.* **1987**, *117*, 567.
(13) Lenz, R. W. *Farady Disc. Roy. Soc.* **1985**, *79*, 21.
(14) Roviello, A.; Sirigu, A. *Gazz. Chim. Ital.* **1979**, *107*, 333.
(15) Sikkema, D. J.; Hoogland, P. *Polymer* **1986**, *27*, 1443.
(16) ten Bosch, A.; Maissa, P.; Sixou, P. *Phys. Lett.* **1983**, *94*(A) 298; *J. Chem. Phys.* **1983**, *79*, 3462; *J. Phys. Lett.* **1983**, *44*, L105.
(17) Khokhlov, A. R.; Semenov, A. N. *Stat. Phys.* **1985**, *38*(1/2), 161.

Poly[(ω-carboxy)oligo(oxyethylene) methacrylate] as a New Type of Polymeric Solid Electrolyte for Alkali-Metal Ion Transport

Eishun Tsuchida,* Hiroyuki Ohno, Norihisa Kobayashi, and Hajime Ishizaka

Department of Polymer Chemistry, Waseda University, Tokyo 160, Japan.

Received January 14, 1988; Revised Manuscript Received September 26, 1988

ABSTRACT: Alkali-metal salts of (ω-carboxy)oligo(oxyethylene) methacrylate (CME$_n$M, M = Li, Na, or K) have been synthesized and polymerized to prepare polymeric solid electrolytes. These polymers have a flexible main chain, an oligo(oxyethylene) side chain for ion conduction, and a carrier ion source in the repeating unit. The conductivity of CME$_7$K homopolymer, 1.1×10^{-7} S/cm at 30 °C, is the highest value reported for a polyelectrolyte "homopolymer" without any additives. This conductivity is attributed to the oligo(oxyethylene) side chain, which facilitates the dissociation of the alkali-metal carboxylate. The temperature dependence of ionic conductivity is not linear, suggesting that conduction occurs by the WLF mechanism. Vogel–Tammann–Fulcher plots are linear when the standard temperature is defined as $T_g - 50$ °C. The differences in conductivity of P(CME$_7$M) with different cations at the same ΔT from T_g are attributed to differences in ion–dipole interaction forces and in dissociation energy of the electrolyte. WLF plots of the conductivity of P(CME$_n$M) are independent of cation species and show a standard curved line, suggesting that carrier ions do not migrate naked but are bound to polymer segments through ion–dipole interaction forces. It is suggested that ion migration is controlled primarily by segmental motion of the polymer rather than by the interaction between cation and ether oxygen.

Introduction

Polymeric solid electrolytes with high ionic conductivity are of interest for theoretical and basic research as well as for applications in novel devices. Research on polyether/inorganic salt hybrids has been aimed at achieving higher conductivity and analyzing the ionic conduction mechanism.[1-9] These polymeric solid electrolytes containing LiClO$_4$ have ionic conductivities of 10^{-6}–10^{-9} S/cm at 25 °C. We have reported an ionic conductivity as high as 10^{-5} S/cm in poly[oligo(oxyethylene) methacrylate]/LiX.[10-12] This ionic conductivity was attributed to the flexible oligo(oxyethylene) segment with a lower T_g than crystalline poly(oxyethylene). Comblike polymers containing oligo(oxyethylene) chains have been used as matrix polymers, and their hybrids with inorganic salts showed similar conductivities.[13-16]

These hybrid polymeric solid electrolytes do not prevent the migration of counterions. Accordingly, a significant decrease in ionic conductivity occurs under continued dc polarization even when alkali-metal nonblocking electrodes are used. It appears that ion pairs are localized near the anode. This localization could increase the T_g of the microenvironment in the polymeric solid electrolyte, thus blocking ion migration and preventing further supply of alkali-metal cations from the anode. This decrease in conductivity bars the use of such electrolytes in devices driven under dc polarization and points to the need for a matrix in which only cation migration is allowed.

There are three approaches to single-ion conduction in a polymer matrix. (1) Blends of polyelectrolyte salts with soft segments such as poly(oxyethylene), in which countercations become mobile,[17,18] are one approach. This selective ion conduction can be attributed to the relatively larger diffusion coefficient of small counterions than that of the giant polyions. (2) Polyelectrolyte "copolymer" systems that contain units with relatively large segmental motion are another. We have reported on copolymers of oligo(oxyethylene) methacrylate and alkali-metal methacrylates as polymeric solid electrolytes that have a carrier ion source and a low T_g matrix and that show high ionic conduction without any additives.[19-21] (3) Polyelectrolyte "homopolymers" are a third approach. We report here the synthesis of alkali-metal salts of (ω-carboxy)oligo(oxyethylene) methacrylate and the preparation of polymeric solid electrolytes from them by polymerization.

Experimental Section

Materials. (ω-Carboxy)oligo(oxyethylene) Methacrylate (CME$_n$H). (ω-Hydroxy)oligo(oxyethylene) methacrylate (Blenmer, Nippon Oil & Fats Co., Ltd.) (20 g for n = 3, 30 g for n = 7) and NaHCO$_3$ (8 g) were dissolved in 500 mL of distilled water. This solution was vigorously stirred with 6 g of 10% platinum-on-carbon catalyst while oxygen was bubbled through. The reaction temperature was maintained under 40 °C to avoid spontaneous polymerization. After 12 h, the catalyst was filtered out and washed well with distilled water to collect monomers. The resulting aqueous solution was adjusted to pH 2 with hydrochloric acid to remove carbonate ion, and the pH was then increased to 8 with aqueous lithium hydroxide solution. The solution was washed with chloroform (500 mL × 6) to remove the unreacted Blenmer. The pH of the solution was again changed to 2, and CME$_n$H was extracted with chloroform. The extract was diluted

0024-9297/89/2222-1771$01.50/0

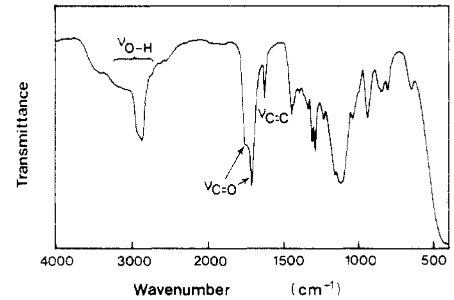

Figure 1. IR spectrum of CME_3H with NaCl plate.

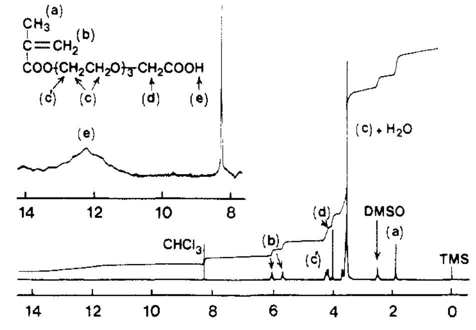

Figure 2. ^1H NMR spectrum of CME_3H in DMSO-d_6 at 25 °C, with TMS as internal reference.

with chloroform to 20 wt % monomer concentration and stored at −20 °C for one day to convert residual water to ice, which was removed by filtration. The structure was confirmed by IR spectroscopy (Figure 1) and ^1H NMR spectroscopy in $(CH_3)_2SO$-d_6 (Figure 2): ^1H NMR 1.9 (3 H, CH_3), 3.6 (OCH_2), 4.0 (2 H, OCH_2CO_2), 4.2 (2 H, CO_2CH_2), 5.5, 6.1 (2 H, $C{=}CH_2$), 12.5 (1 H, CO_2H). Alkali-metal salts (CME_nM, M = Li Na, or K) were prepared by neutralization of CME_nH with alkali-metal hydroxides in methanol.

Homogeneous polymerization of CME_nM was carried out in methanol with azobis(isobutyronitrile) (0.2 mol %) initiator under nitrogen at 60 °C for 40 h. The polymer P(CME_nM) was precipitated twice from benzene and then dried in vacuo at 60 °C for 1 day. A methanol solution of P(CME_nM) was cast on a Teflon plate, and the solvent was evaporated under dry nitrogen flow over P_2O_5 for 20 h at 60 °C. The film was dried at 80 °C in vacuo for 40 h.

Cast polymerization was carried out by casting a 20 wt % methanol solution of CME_nM on a Teflon plate and evaporating the solvent under dry nitrogen flow over P_2O_5 for 24 h at 60 °C. The film was dried in vacuo at 80 °C for 48 h.

The films were generally 100–200 μm thick.

Methods. All measurements were carried out in a drybox filled with dry argon.

The average molecular weight of P(CME_nM), obtained by homogeneous polymerization, was determined by gel permeation chromatography with tetrahydrofuran as eluent.

Ionic conductivity measurements (ac 1 V) were carried out with a Yokogawa–Helewett-Packard multifrequency LCR meter (Model 4274A) over the frequency range 10^2–10^5 Hz. Disk samples (10-mm diameter) were sandwiched between metallic lithium or stainless steel electrodes. The ac ionic conductivity was calculated from a complex impedance plot[22] with computer curve fitting. The temperature dependence of conductivity was determined under dry argon over the range 0–100 °C.

Metallic lithium or stainless steel electrodes were also used for dc (3 V) conductivity measurements with a Kikusui dc power supply (Model PAC 7-10), a Kikusui millivolt ammeter (Model 115), and a Keithley solid-state electrometer (Model 610C). Details of the instrumentation were described previously.[10]

The thermal history of the polymeric film was determined with a differential scanning calorimeter (SEIKO, Model SSC-580, DSC-10) under dry argon. The scanning speed was 8 °C/min, and six measurements were made on each sample. The T_g was taken as the lower intersection point of the base line with the extrapolated slope of the thermogram.

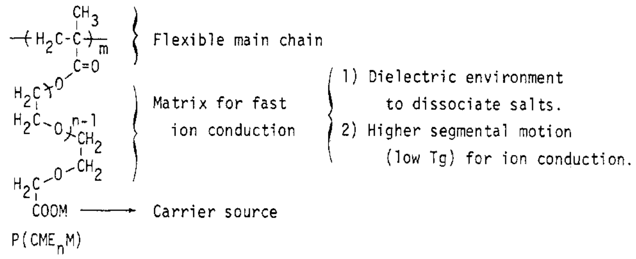

Figure 3. Structure of P(CME_nM) and expected roles of segments.

Table I
Relation between T_g and Ionic Conductivity of P(CME_nM) Films

polymer	polymerization	salt	conductivity, S/cm (30 °C)	T_g, °C
P(CME_3M)	cast	Li	7.9×10^{-11}	32
		Na	7.1×10^{-8}	−22
		K	2.2×10^{-8}	−9
	homogeneous	Li	$<10^{-11}$	32
		Na	3.2×10^{-11}	27
		K	2.0×10^{-10}	33
P(CME_3M)	cast	Li	3.2×10^{-9}	−44
		Na	3.1×10^{-8}	−43
		K	1.7×10^{-7}	−39
	homogeneous	Li	4.3×10^{-10}	−23
		Na	2.2×10^{-8}	−24
		K	1.1×10^{-7}	−24

X-ray diffraction patterns of the films were determined with an X-ray diffractometer (Rigaku Denki Co., Ltd., Model 2026) by using the reflection method and Cu Kα radiation. The films were mounted on a glass sample rest, and the diffraction pattern was obtained with the 2θ–θ scan mode.

The morphology of the film was studied on the sample rest with a polarizing microscope (SUR-UT, Nikon Co., Ltd.).

IR spectroscopy was carried out with an IR spectrometer (Japan Spectroscopic Co., Ltd., Model IR 810), using KBr pellets for solid samples and a cell with a NaCl window for solutions.

Results and Discussion

Spectroscopic evidence confirmed that the terminal OH group in (ω-hydroxy)oligo(oxyethylene) methacrylate had been oxidized to CO_2H. The IR spectrum of CME_3H shows $\nu_{C=O}$ (CO_2H) at 1750 cm^{-1} and a broad peak at 2700–3200 cm^{-1} for ν_{OH} (CO_2H). The ^1H NMR spectrum of CME_3H no longer had a peak at 2.8 ppm corresponding to the terminal hydroxy proton but rather a new broad peak at about 12 ppm, attributed to a carboxylic acid proton. The data suggest that only the terminal OH group has been oxidized. These monomers have both a carrier source (dissociable group) and the oligo(oxyethylene) moiety for ion conduction (Figure 3). In addition, their polymers have a flexible main chain.

The ionic conductivities and T_g values for P(CME_nM) films are summarized in Table I. P(CME_nM) films obtained by homogeneous polymerization are transparent and soluble in methanol. After the terminal −COOM groups of P(CME_nM) were esterified to prepare methyl ester with 10% HCl/methanol solution, the average molecular weight of the polymer was estimated to be over 60 000 (polystyrene standard). On the other hand, the films obtained by cast polymerization were insoluble in organic solvents. P(CME_3M) film was glassy and rigid, in contrast to P(CME_7M), reflecting a high T_g. Both films were confirmed to be fully amorphous by DSC and X-ray diffraction, whereas high molecular weight PEO/alkali metal salt hybrids with concentration ratios of 7/1 or 3/1 were crystalline at ambient temperature. Poly[oligo(oxyethylene) methacrylate] with a terminal hydroxy or methyl

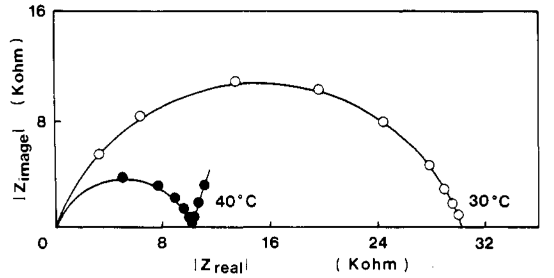

Figure 4. Complex impedance plots at 30 and 40 °C of P-(CME_7K) obtained by homogeneous polymerization.

ester group has an amorphous structure, which is retained after the introduction of ionic groups on the polymer chain. The polymers showed no endothermic or exothermic change over the temperature range −150 to 120 °C, except the T_g. Above 150 °C, an exothermic decomposition occurred in all samples similar to that observed with poly-[oligo(oxyethylene) methacrylate-*co*-alkali-metal methacrylate].[21] Measurement of the ac conductivity of P(CME_nM) films showed them to be ohmic conductors under an applied voltage up to 5.0 V at 30 °C.

Complex impedance plots[22] for P(CME_7K) films with stainless steel electrodes at 30 and 40 °C are shown in Figure 4. Only one semicircular arc passing through the origin is observed in this frequency range at 30 °C, although the curve deviates from the arc at lower frequencies with increasing temperature. These results indicate that the equivalent circuit in this system involves polarization processes in the film bulk and at the film/electrode interface. According to this interpretation, the bulk impedance of the films is taken as the intersection of the left arc with the abscissa, and this value is used to calculate the normalized ac ionic conductivities of P(CME_nM). The conductivity of homogeneously polymerized P(CME_7M) at 30 °C, 1.1×10^{-7} S/cm, while not remarkable, is the highest value reported for a polyelectrolyte "homopolymer" without additives.

The T_g values of P(CME_3M) (~30 °C) and P(CME_7M) (~ −24 °C) were independent of the cation species. In contrast, the T_g values of hybrid polymeric solid electrolytes are considerably affected by cation species and salt content because of ion–dipole interaction between ions and polymer. This difference presumably reflects that the increase of T_g is found even by the introduction of ionic groups covalently on the polymer chain, as seen in Ionomer. The fact that the T_g of P(CME_7M) is lower than that of P(CME_3M) is attributed to the lower electrolyte concentration in P(CME_7M). On the other hand, P(CME_7M) films have higher conductivity than P(CME_3M) for the same cation species. The conductivity is a function of the product of total number of carrier ions and carrier mobility. The electrolyte contents of P(CME_7M) and P(CME_3M) are 14.2 and 33.3 mol % per oxyethylene unit, and the absolute electrolyte concentration of P(CME_3M) is higher than that of P(CME_7M). The effect of segmental motion of the polymer matrix, which is correlated with carrier mobility, is dominant for ion conduction in this electrolyte concentration range. The conductivity of P(CME_nM) increases with the ionic radius of the cation (Table I), presumably reflecting the lower dissociation energy of the electrolyte salt. The electrolytes in P(CME_nM) have same anion and exist in the same oligo(oxyethylene) matrix, and their dissociation energy increases in the order K < Na < Li. The conductivity of poly(oxyethylene), with an average molecular weight of 400/alkali-metal thiocyanate fluid solution, increases in the order Li < Na < K.[11] Since the electrolytes in this system also exist in the same oligo(oxyethylene) environment, the dissociation tendency in P(CME_nM) is in the order Li < Na < K. Accordingly, we conclude that P(CME_nK) has the highest conductivity among these homopolymers.

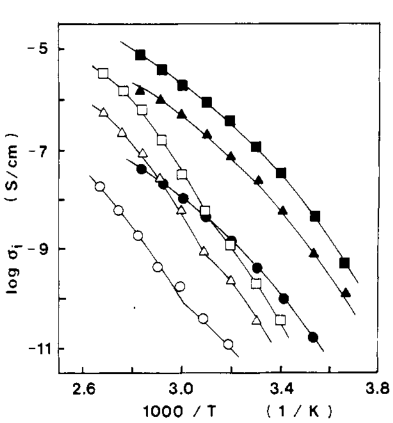

Figure 5. Temperature dependence of the ac ionic conductivity of P(CME_nM) films obtained by homogeneous polymerization: open symbols, P(CME_3M); solid symbols, P(CME_7M); circle, Li; triangle, Na; square, K.

CME_nM polymerizes spontaneously on heating above 60 °C, and films a few micrometers thick are prepared by cast polymerization. P(CME_nM) films so prepared had higher conductivity than P(CME_nM) films prepared by homogeneous polymerization (Table I). Although the degree of polymerization is limited in homogeneous polymerization, the cast-polymerized films are believed to have a broader molecular weight distribution. Low molecular weight polymer fractions in the cast-polymerized films might provide a better matrix for ionic conduction because of low viscosity and high mobility. There was no apparent relationship between the conductivity of cast-polymerized P(CME_nM) and cation species, possibly because of different amounts of oligomer in different films. The oligomer content of the cast-polymerized films is probably responsible for their lower T_g.

In order to confirm that anion migration does not contribute to the conductivity of the cast-polymerized P(CME_3Li) film, the time dependence of dc ionic conductivity is measured with lithium or stainless steel electrodes. With the latter, the conductivity decreased to half the initial value after 20 min at 80 °C. This result is attributed to polarization of the cation at the polymeric solid electrolyte/electrode interface, because no carrier ion is supplied from ion-blocking electrode to electrolyte. On the other hand, the conductivity measurement with lithium electrodes showed excellent stability at 3 V, indicating that no anion polarization was occurring. This suggests that P(CME_3Li) is the only cation conductor.

The temperature dependence of ionic conductivity in homogeneously polymerized P(CME_nM) was determined over the range 0–100 °C (Figure 5). The inflection in the curve for P(CME_3M) coincides approximately with the T_g of P(CME_3M). The temperature dependence above the inflection point was not linear, indicating that the ionic conduction followed the Williams–Landel–Ferry (WLF) mechanism.[23] This result suggests that carrier ions migrate through polymer segmental motion with continued ion–dipole interaction. However, Vogel–Tammann–Fulcher plots, which are known to describe transport properties in a viscous matrix, show good linearity when the standard temperature is defined as T_g − 50 °C (Figure 6).[24] This result is consistent with the configurational entropy.[25] These results suggest that ionic conduction is considerably affected by the segmental motion in P(CME_nM).

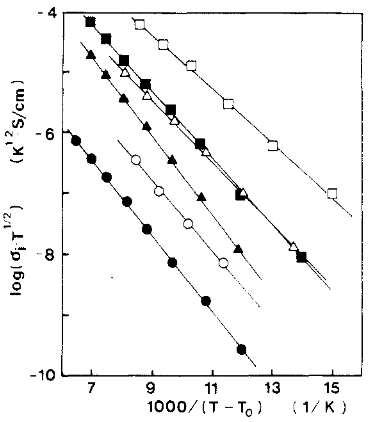

Figure 6. Vogel–Tammann–Fulcher plots for P(CME_nM) films obtained by homogeneous polymerization: open symbols, P(CME_3M); solid symbols, P(CME_7M); circle, Li; triangle, Na; square, K.

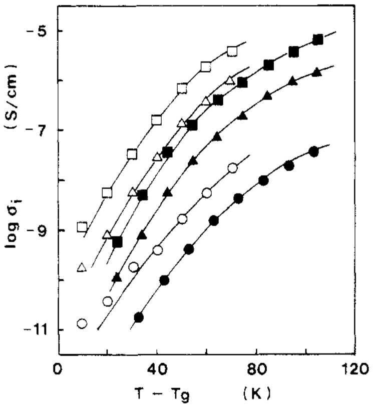

Figure 7. Relation between $T - T_g$ and the conductivity of P(CME_nM) films obtained by homogeneous polymerization: open symbols, P(CME_3M); solid symbols, P(CME_7M); circle, Li; triangle, Na; square, K.

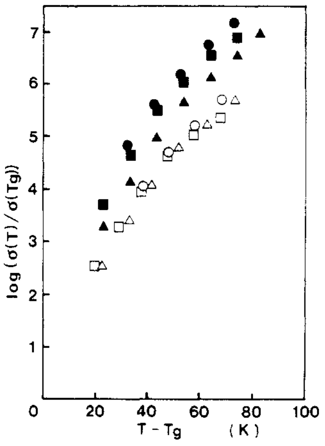

Figure 8. WLF plots of the conductivity of P(CME_nM) films obtained by homogeneous polymerization: open symbols, P(CME_3M); solid symbols, P(CME_7M); circle, Li; triangle, Na; square, K.

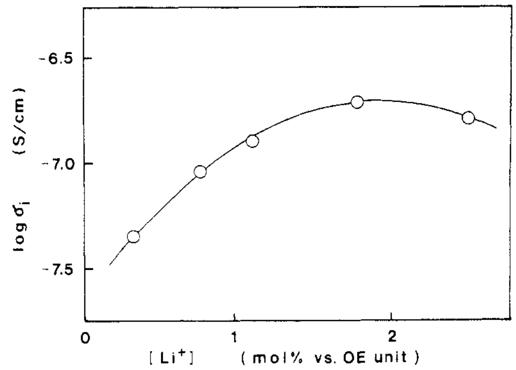

Figure 9. Electrolyte concentration (CME_3Li mole fraction) dependence of the conductivity of P(CME_3Li-MEO_7) films obtained by cast polymerization.

The relationship between $T - T_g$ and conductivity of P(CME_nM) is shown in Figure 7. Conductivity can be expressed as

$$\sigma = ne\mu \qquad (1)$$

where n is the total number of carrier ions, e is the elementary electric charge, and μ is the carrier mobility. The different values of this relation for different polymers appear to reflect differences in the number of carriers, which is determined by the dissociation energy of the electrolyte. However, the differences in conductivity with different cations are too large to be explained only by the differences in electrolyte dissociation and probably reflect differences in carrier mobility. Although cation migration is directly related to polymer segmental motion, this segmental motion is almost the same in each system at $T - T_g$. Accordingly, in a given polymer matrix, carrier mobility at the same ΔT from T_g depends upon the interaction force between ions and dipoles. This interaction force decreases in the order Li > Na > K because the charge density on ions decreases in that order. Carrier mobility in the potassium polymers is higher than that in sodium or lithium polymers. Consequently, the differences in conductivity with different cation species at the same ΔT from T_g reflect both differences in ion–dipole interaction forces and differences in electrolyte dissociation energy.

Although the conductivity of P(CME_3M) is much lower than that of P(CME_7M) at the same temperature, P(CME_3M) films show higher apparent conductivity than P(CME_3M) with the same cation species at the same ΔT from T_g. Since P(CME_3M) and P(CME_7M) with the same cation species have essentially the same segmental motion of the polymer matrix and the same ion–dipole interaction force at the same ΔT from T_g, the conductivity difference is attributed to the higher concentration of charge in P(CME_3M).

WLF plots of the conductivity of P(CME_nM) obtained by homogeneous polymerization (Figure 8) are independent of cation species and on a standard curved line. Thus it appears that carrier ions do not move naked but are surrounded by polymer segments through ion–dipole interaction. We therefore suggest that ion migration is controlled primarily by the energy of segmental motion in the polymer matrix rather than by interaction between cations and ether oxygens.

In an attempt to increase conductivity by increasing the segmental motion of the polymer matrix, we prepared a copolymer of oligo(oxyethylene) methacrylate (MEO_7) with the lithium salt of (ω-carboxy)oligo(oxyethylene) methacrylate (P[CME_3Li)-*co*-(MEO_7)]) by cast polymerization. The relationship between the conductivity of this copolymer and its salt content (Figure 9) shows a maximum conductivity of 2 × 10^{-7} S/cm at a lithium ion concentration of 1.8 mol %. This value is about 10^4 times higher than that of cast-polymerized P(CME_3Li). The T_g of the copolymer at this lithium ion concentration is −59 °C. These results support our suggestion that ionic conductivity should be increased by increasing segmental motion in the polymer matrix.

Acknowledgment. This work was partially supported by a Grant-in-Aid for Scientific Researches on the Priority

Area of Macromolecular Complexes from the Ministry of Education, Science, and Culture, Japan.

Registry No. (CMe$_3$Li)(MEO$_7$) (copolymer), 118400-61-6; $H_2C{=}C(CH_3)CO_2(CH_2CH_2O)_3CH_2CO_2Li$ (homopolymer), 118400-50-3; $H_2C{=}C(CH_3)CO_2(CH_2CH_2O)_3CH_2CO_2K$ (homopolymer), 118400-52-5; $H_2C{=}C(CH_3)CO_2(CH_2CH_2O)_3CH_2CO_2Na$ (homopolymer), 118400-54-7; $H_2C{=}C(CH_3)CO_2(CH_2CH_2O)_7CH_2CO_2Li$ (homopolymer), 118400-56-9; $H_2C{=}C(CH_3)CO_2(CH_2CH_2O)_7CH_2CO_2K$ (homopolymer), 118400-58-1; $H_2C{=}C(CH_3)CO_2(CH_2CH_2O)_7CH_2CO_2Na$ (homopolymer), 118400-60-5; CME$_3$H, 118457-79-7.

References and Notes

(1) Wright, P. V. *Br. Polym. J.* **1975**, *319*, 137.
(2) Papke, B. L.; Ratner, M. A.; Shriver, D. F. *J. Phys. Chem. Solid* **1981**, *42*, 493.
(3) Berthier, C.; Gorecki, W.; Minier, M.; Armand, M. B.; Chabagno, J. M.; Riguad, P. *Solid State Ionics* **1983**, *11*, 91.
(4) Dupon, R.; Papke, B. L.; Ratner, M. A.; Whitmore, D. H.; Shriver, D. F. *J. Am. Chem. Soc.* **1982**, *104*, 6247.
(5) Weston, J. E.; Steel, B. C. H. *Solid State Ionics* **1982**, *7*, 81.
(6) Killes, A.; Le Nest, J. F.; Gandini, A.; Cheradame, H. *Macromolecules* **1984**, *17*, 63.
(7) Watanabe, M.; Ikeda, J.; Shinohara, I. *Polym. J.* **1983**, *15*, 65, 175.
(8) Yang, L. L.; McGhie, A. R.; Farrington, G. C. *J. Electrochem. Soc.* **1986**, *133*, 1380.
(9) Tsuchida, E.; Ohno, H.; Tsunemi, K.; Kobayashi, N. *Solid State Ionics* **1983**, *11*, 227.
(10) Kobayashi, N.; Uchiyama, M.; Shigehara, K.; Tsuchida, E. *J. Phys. Chem.* **1985**, *89*, 987.
(11) Kobayashi, N.; Ohno, H.; Tsuchida, E. *J. Chem. Soc. Jpn.* **1986**, 441.
(12) Kobayashi, N.; Ohno, H.; Tsuchida, E.; Hirohashi, R. *Koubunshi Ronbunshu* **1987**, *44*, 317.
(13) Blonsky, P. M.; Shriver, D. F.; Austin, P.; Allcock, H. R. *J. Am. Chem. Soc.* **1984**, *106*, 6854.
(14) Bannister, D. J.; Davies, G. R.; Word, I. M.; McIntyre, J. E. *Polymer* **1984**, *25*, 1600.
(15) Xia, D. W.; Soltz, D.; Smid, J. *Solid State Ionics* **1984**, *14*, 85.
(16) Le Mehaute, A.; Crepy, G.; Marcellin, G.; Hamaide, T.; Guyot, A. *Polym. Bull.* **1985**, *14*, 233.
(17) Bannister, D. J.; Davies, G. R.; Word, I. M.; McIntyre, J. E. *Polymer* **1984**, *25*, 1291.
(18) Hardy, L. C.; Shriver, D. F. *J. Am. Chem. Soc.* **1985**, *107*, 3823.
(19) Kobayashi, N.; Uchiyama, M.; Tsuchida, E. *Solid State Ionics* **1985**, *17*, 307.
(20) Kobayashi, N.; Hamada, T.; Ohno, H.; Tsuchida, E. *Polym. J.* **1986**, *18*, 661.
(21) Tsuchida, E.; Kobayashi, N.; Ohno, H. *Macromolecules* **1988**, *21*, 96.
(22) Cole, K. S.; Cole, R. H. *J. Chem. Phys.* **1941**, *9*, 341.
(23) Williams, M. L.; Landel, R. F.; Ferry, J. D. *J. Am. Chem. Soc.* **1955**, *77*, 3701.
(24) (a) Vogel, H. *Phys. Z.* **1921**, *22*, 645. (b) Tammann, V. G.; Hesse, W. Z. *Anorg. Allg. Chem.* **1926**, *156*, 245. (c) Fulcher, G. C. *J. Am. Ceram. Soc.* **1925**, *8*, 339.
(25) Wintersgill, M. C.; Fontanella, J. J.; Smith, M. K.; Greenbaum, S. G.; Adamic, K. J.; Andeen, C. G. *Polymer* **1987**, *28*, 633 and references therein.

Partition Coefficients of Rigid, Planar Multisubunit Complexes in Cylindrical Pores

Ruth E. Baltus

Department of Chemical Engineering, Clarkson University, Potsdam, New York 13676.

Received July 25, 1988; Revised Manuscript Received September 20, 1988

ABSTRACT: A theoretical investigation of the equilibrium partition coefficient of planar multisubunit model structures in cylindrical pores was undertaken. These models are rigid complexes assembled from identical spherical subunits. Model structures containing two to eight subunits were investigated. The effective hydrodynamic radius was found to reasonably characterize the partitioning properties of the multisubunit models; however, the partition coefficient for each multisubunit structure was significantly smaller than that for a spherical solute with the same hydrodynamic radius. The partitioning characteristics of the multisubunit complexes were comparable to those predicted for oblate ellipsoid particles with an axial ratio of ~0.01–0.05, a ratio which is considerably smaller than the ratio of the smallest to largest dimension of these structures. The results show that the partition coefficient does not correlate well with molecular radius, which is defined as the radius of a sphere with the same volume as the multisubunit complex.

Introduction

When the size of a solute is comparable to the pore size through which it is diffusing, reduced diffusion rates are observed. This phenomenon is called hindered diffusion and results from the combination of two effects: one is an equilibrium effect and the other a transport effect. The equilibrium partitioning of solute molecules between the pore and bulk solutions results in an intrapore concentration driving force which is less than the driving force based on bulk solution concentrations. The proximity of the pore wall causes an increase in the frictional resistance experienced by the solute as it diffuses through the pore. This description of the physics governing hindered diffusion becomes more complicated when one includes the influence of long-range solute–pore wall interactions. An understanding of the equilibrium and transport properties of macromolecules in porous media is important in applications such as size exclusion chromatography, membrane separation processes, and heterogeneous catalysis.

The equilibrium partitioning of solute molecules between pore and bulk solutions is described by using a partition coefficient, defined as the ratio of pore to bulk solution concentrations. A general expression for the partition coefficient, K, for rigid molecules based on statistical mechanics is[1]

$$K = \frac{C_p}{C_b} = \frac{\int_{\mathbf{x}}\int_{\Psi} \exp[-E(\mathbf{x},\Psi)/kT]\,\mathrm{d}\mathbf{x}\,\mathrm{d}\Psi}{\int_{\mathbf{x}}\int_{\Psi} \mathrm{d}\mathbf{x}\,\mathrm{d}\Psi} \qquad (1)$$

where C_p is the solute concentration in the pore and C_b is the solute concentration in the bulk solution. Here, $\mathbf{x}$ and Ψ represent generalized position and molecular orientation coordinates, respectively. The potential energy of a solute molecule in the pore is represented by $E(\mathbf{x},\Psi)$; $E = 0$ in bulk solution.

Giddings et al.[1] evaluated the integrals in eq 1 for rigid molecules limited to steric or "hard-wall" interactions with the pore wall. This hard-wall potential field results in E

0024-9297/89/2222-1775$01.50/0